Received: 13 July 2022 | Revised: 29 September 2022 | Accepted: 12 December 2022

DOI: 10.1002/ese3.1378

ORIGINAL ARTICLE

A novel combo-transmission system of cold energy and electricity for aluminium profile production: Using liquid nitrogen and superconductor technologies

Xiaoyuan Chen[1] | **Qiang Li**[1] | **Shan Jiang**[1] | **Mingshun Zhang**[1] | **Lin Fu**[2,3] | **Boyang Shen**[2,4]

[1]School of Engineering, Sichuan Normal University, Chengdu, China

[2]Department of Engineering, University of Cambridge, Cambridge, UK

[3]VLSI Research Europe, Cambridge, UK

[4]Clare Hall, University of Cambridge, Cambridge, UK

Correspondence
Lin Fu and Boyang Shen, Department of Engineering, University of Cambridge, Cambridge CB3 0FA, UK.
Email: lin.fu.2017@outlook.com and bs506@cam.ac.uk

Funding information
Sichuan Science and Technology Program, Grant/Award Number: 2022YFG0304

Abstract

Aluminium production needs the most energy-intensive technologies among all the metal processing sectors. During the process of aluminium profile extrusion, the whole production line needs bulk electricity, and the mold inside the extrusion equipment needs robust cold energy for rapid cooling of the metal surface. This paper presents a new combo-transmission that can simultaneously deliver cold energy together with electricity to the aluminium profile extrusion line. Thanks to the superiority of virtually zero loss and compact size, the powerful superconducting cable is used to replace the conventional copper cable. The entire superconducting cable assembly is fully installed into a cryogenic pipeline and cooled by liquid nitrogen at 77 K. In addition to keeping a favourable cryogenic environment for the superconducting cable, liquid nitrogen can also provide a large amount of cold energy for cooling the metal surface. For a typical 100 MN aluminium extrusion production line, the design and optimization of 10 kA class superconducting cable with the pipeline cooling system for aluminium production are presented in detail. The simulation results and comparisons show that the total energy loss of superconducting transmission is about 46% of conventional copper cable, and the energy saved in a year can be up to about 240.6 MWh. Moreover, the net profit increases almost linearly along with the increases of the extrusion speed when the liquid nitrogen cooling is applied to the 100 MN production line. For the case of 23% increase in extrusion speed, the net profit can be up to 1.48 M$ in a year. Overall, the novel design, technical evaluation, and economic analysis of the combo-transmission system (cold energy + electricity) can provide a promising solution for future high-dense aluminium production sectors.

KEYWORDS
aluminium production, die cooling, liquid nitrogen, superconducting power cable, superconductor

This is an open access article under the terms of the Creative Commons Attribution License, which permits use, distribution and reproduction in any medium, provided the original work is properly cited.
© 2022 The Authors. *Energy Science & Engineering* published by the Society of Chemical Industry and John Wiley & Sons Ltd.

1 | INTRODUCTION

Aluminium is the most abundant metal in the Earth's crust, and the second most widely used material after steel. Meanwhile, aluminium production needs the most energy-intensive technologies among all the metal processing sectors. A typical aluminium production requires almost 200 GJ/t (gigajoules per ton),[1] which is also equivalent to 4.78 toe/t (tonnes of oil equivalent per ton),[2] or 55,600 kWh/t (kilowatt-hour per ton).[3] The energy consumption of aluminium production is almost 10 times of that required for steel production. Therefore, reducing the energy consumption in aluminium production, and increasing the energy efficiency of production, can be the most effective way to achieve low-carbon productions of major metals.

China is the world's largest producer and consumer of aluminium. According to the data of the National Bureau of Statistics (China),[4] in 2021, the production of alumina, electrolytic aluminium, and aluminium materials was 77.48, 38.5, and 61.05 million tons, respectively, with a year-on-year increase of 5%, 4.8% and 7.4%. At present, the annual power consumption of the whole aluminium industry exceeds 500 billion kWh,[5] which is absolutely a huge amount and accounts for about 6.8% of the total power consumption of the local community. The electricity fee accounts for more than 40% of the production cost of electrolytic aluminium, so it is urgent to find new technologies for energy-saving transformation.

As one of the main processing materials, aluminium profiles can be divided into two categories: architectural aluminium profiles, and industrial aluminium profiles. Aluminium profiles are widely used for building construction because of their decent decoration, excellent processability and recyclability. Meanwhile, with the advantages of one-time extrusion, strong mechanical properties, good thermal conductivity and high specific strength, it is also widely used in transportation, light industry, petroleum, chemical industry, and so forth. According to the data from China Nonferrous Metals Industry Association,[6] the national aluminium output in 2021 was about 20.59 million tons, a year-on-year increase of 2.3%, including 13.8 million tons of building aluminium profiles, accounting for 67.02% of the aluminium profile output, and 6.79 million tons of industrial aluminium profiles, accounting for 32.98% of the aluminium profile output.

Extrusion is one of the most used forming processes for aluminium and its alloys.[7,8] How to ensure the quality of aluminium profile, shorten the production time, and improve the service life of die sets are the core issues in the extrusion process. The increase of temperature may result in surface defects on the extrudate, for example, hot cracks or grain coarsening after extrusion.[9] This excessive temperature (exit profile) can cause several aesthetic defects or cracks on the profile surface, resulting in the scrap of the products or in the reduction of the service life of the tools.[10–13] This excessive temperature also strongly increases with extrusion speed, which limits the maximum productivity.[14]

To solve these problems, water cooling, air cooling and other methods were used to cool die sets in the past,[15,16] but the water cooling die will form coarse grains at the outer edge of the profile, and weaken the mechanical performance of the profile.[17] The air cooling die will have great defects on the profile and a large amount of adhesion materials on the surface.[18] Both will increase the extrusion force of the aluminium extruder and significantly enlarge the mechanical load of die sets and machines.[16]

The liquid nitrogen (LN_2) cooling technology for extrusion dies has become a significant development over recent years.[19,20] LN_2 cooling die technology can effectively solve the problem of the die temperature rise during extrusion. The modulation system accurately controls the flow of liquid nitrogen according to the temperature detected by the infrared thermometer at the extrusion end of the die, so as to control the flow of liquid nitrogen at the outlet of the final die. The whole loop system accurately controls the temperature of the extrusion die, and realizes the constant-temperature extrusion. The inert nitrogen formed can effectively cool down the die, which is able to protect the high-temperature profile and completely avoids surface oxidation, so as to improve the surface quality of aluminium profile and improve the service life of the die.[21–23]

In recent years, many scholars have studied the technology of die cooling using liquid nitrogen. It is a well-known approach to increase the process speed of aluminium profile, reduce the temperature of die and tools, and improve the surface quality of extruded profile.[18,24] presented a general but simple on-line simulation tool to determine the optimal process conditions for isothermal extrusion.[19] tested the effects of different nitrogen flows on the process load, and the temperature evolution of the die and profile exit on, for a complex industrial hollow profile made by AA6060. Liquid nitrogen die cooling technology can improve the surface quality of AA6060 aluminium profile and make the surface smoother, and meanwhile, almost no peak defects appear on the surface.[25–27] presented a finite element method (FEM) to cool down channels, which is mainly for die plastic injection molding and casting applications. The capability of nitrogen cooling within a conformal channel was experimentally and numerically

assessed, for the extrusion of AA6063 aluminium and ZM21 magnesium alloys.[28] A platform for testing the liquid nitrogen cooling for multi-die design was proposed.[29] To provide extruders and die manufacturers with a numerical tool particularly for the thermal distributions of dies, a FEM model for the extrusion process with the liquid nitrogen cooling system was developed.[30] A numerical model of AA6060 extrusion process was carried out to predict and optimize the nitrogen cooling effect in the die.[31] A numerical model is used to optimize the channel design in terms of the cooling efficiency, die heat balance, and reduction of liquid nitrogen consumption.[32] To efficiently install the cooling channels as close as possible to the bearing region, conformal cooling channels manufactured by selective laser melting (SLM) are implemented in the die designs.[33–35]

Based on our best search of the literature, most studies focus on theoretical analysis, technical simulation, and performance improvement of liquid nitrogen cooling technology for aluminium profile extrusion. However, there is no comprehensive techno-economic study on the liquid nitrogen cooling technology, from the perspective of the energy efficiency and productivity of an entire workshop for aluminium profile extrusion.

Meanwhile, due to the significant electricity consumption in the workshops for aluminium profile extrusion, the electric losses in the power cables cannot be neglected. Conventional copper power cables with high-current and low-voltage have huge electric losses, which also cause the over-heat of power cables, and can lead to safety issues such as insulation breakdown and fire hazard. If replacing the conventional copper power cables with the virtually zero-resistance superconducting power cables,[36,37] the workshops for aluminium profile extrusion can realize the large-capacity and low-loss energy distribution, and prevent the safety issues above. Superconducting power cables have shown great advantages for those high-current low-voltage industrial power sectors. Nowadays there are numerous prototypes of superconducting magnetic energy storage devices and superconducting power cables, with their economic evaluations.[38–40] Concerning the structural design, a considerable amount of high-current cables have been demonstrated globally, which include the simply-stacked conductor (SSC) cable,[41] twisted stacked-tapes cable (TSTC) cable,[42] quasi-isotropic strand (QI-S) cable,[43] conductor on round core (CORC) cable,[44] Roebel assembled coated conductor (RACC) cable,[45] and round strand (RS) cable.[46] However, in respect of the wide uses in actual engineering scenarios, one side-issue is that superconducting cables need cryogenic working conditions (e.g., liquid nitrogen), and this will also introduce extra operation costs to build such cryogenic systems in aluminium workshops.

Fortunately, liquid nitrogen can be used as the coolant to solve the temperature rising issue and improve the productivity of the aluminium profile extrusion in workshops. Accordingly, there should be large-size liquid nitrogen tanks and pipelines transporting liquid nitrogen into workshops.

For this particular matter, this article proposes a novel scheme to transport the liquid nitrogen and electricity into an aluminium workshop at the same time. The liquid nitrogen tank can be installed beside the low-voltage electricity distribution station, and the superconducting cable can be installed inside the cryogenic liquid nitrogen pipelines. Overall, this new scheme can simultaneously transport and supply 'cold energy + electricity' to the devices working for aluminium profile extrusion, which is able to greatly improve the energy efficiency and productivity of the workshop.

2 | PRINCIPLE AND TECHNOLOGICAL PROCESS OF ALUMINIUM PROFILE EXTRUSION

The production of aluminium extrusion mainly requires the aluminium extruder, heating furnace, cooling bed, aging furnace, die furnace, tractor and other equipment. The production process in Figure 1 includes six phases: preheating, extrusion, quenching and cutting, straightening and sizing, aging hardening and delivery. The details are as follows:

(1) Preheating phase. The aluminium rod is put into the heating furnace for heating. When the temperature reaches 500°C, after holding for one hour the normal production can start. During the same time of heating the aluminium rod, the die is put into the

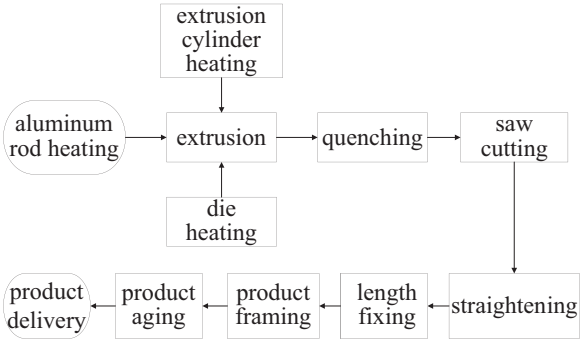

FIGURE 1 Flowchart of aluminium extrusion production

die heating furnace for heating, and the extrusion cylinder is heated by electromagnetic induction, so that the temperature of the die and the extrusion cylinder can both reach 500°C.

(2) Extrusion phase. After the heating and temperature holding processes are completed, the die is put into the die seat of the extruder, and the cut aluminium rod is put into the extruder for extrusion.

(3) Quenching and cutting phase. The traction cutting system includes roller path, tractor, movable cut-off saw and water quenching device. The extruded aluminium rod is pulled by the tractor in the traction cutting system, which will be water-cooled quenched by the water quenching device on the roller path, and then sawed with a fixed length.

(4) Straightening and sizing phase. The aluminium profile is sent to the cooling bed for straightening. The straightened aluminium profile is transported to the complete product area to cut to length.

(5) Aging hardening phase. The cut aluminium profile is loaded into the material frame as required, transported to the aging area, and aged after entering the aging furnace. When the ageing temperature reaches 200°C, the aluminium profile will be kept warm for 2 h, and then wait to leave the aging furnace.

(6) Delivery phase. The aluminium profile product will be packaged and shipped.

3 | SYSTEM DESIGN OF A 100 MN ALUMINIUM EXTRUSION PRODUCTION LINE WITH LIQUID NITROGEN COOLING

As shown in Figure 2, the production line mainly has the heating furnace, extruder, cooling bed, die furnace, aging furnace and other equipment. The heating furnace and die furnace are on the one side of the extruder, while the extruder, cooling bed, lead-out area and aging furnace are arranged horizontally. The entire production line is installed inside a workshop (length 252 m, width 30 m). The electricity distribution station outside the workshop is 10 m long and 5 m wide, which can supply a 380 V AC electric power source. The liquid nitrogen tank and distribution station are 6 m away from the workshop, which supplies liquid nitrogen via cryogenic pipeline into the die system. The 3-phase 380 V AC electric power is delivered via the superconducting cable to the production line for the aluminium profile extrusion. To properly use the existing cryogenic environment, the superconducting cable is installed inside the liquid nitrogen pipelines. Overall, this new scheme can transport and supply liquid nitrogen and electrical power (cold energy + electricity), via multi-energy cryogenic pipelines, into the aluminium extrusion workshop.

The working principle of this combo-transmission system (cold energy + electricity) can be described as follows:

(1) The liquid nitrogen from the tank, which is driven by the cryogenic pump, first enters into the 1st gas-liquid separator installed outside the workshop, and then enters into the 54 m cryogenic pipeline, and after that the liquid nitrogen is delivered to the 2nd gas-liquid separator inside the workshop.

(2) The short copper connector (1 m long) first links the external terminal (room-temperature) of the current leads, and then links the internal terminal with the further high temperature superconducting (HTS) power cable inside the cryogenic pipeline. The length of the HTS power cable is the same as the cryogenic pipeline (both 54 m, the distance between the 1st gas-liquid separator and the 2nd gas-liquid separator).

(3) At the output of the 2nd gas-liquid separator, the separated pure liquid nitrogen flows into the liquid nitrogen valve box through a 6 m soft vacuum

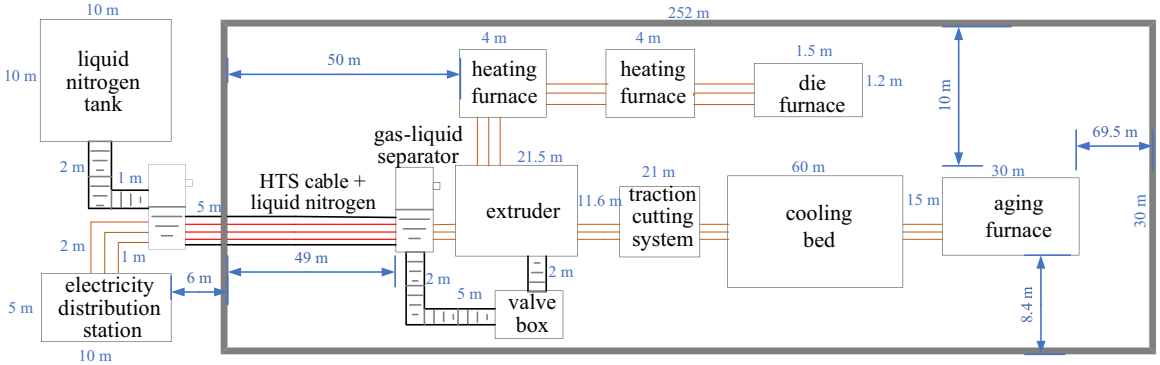

FIGURE 2 Schematic diagram of a 100 MN aluminium extrusion workshop using the combo-transmission system for 'cold energy + electricity'

pipeline. In the real operation, the valve box can use a certain portion and a certain speed to control the flow rate of output liquid nitrogen according to the requirements of customers and aluminium extruders, which can realize the fast cooling of extruders.

(4) The electricity transmitted by the HTS power cable relays to the room-temperature current leads of the 2nd gas-liquid separator, and further passes through a short copper connecter to link the production line of aluminium profile extrusion. This novel process can achieve high-current high-quality electric power transmission with overall ultra-low loss.

It should be noted that the input and output current leads are installed on both two gas-liquid separators. Due to the temperature difference between room and liquid nitrogen, heat leak is inevitable. Furthermore, the process of liquid nitrogen being transferred from the tank, through the cryogenic pipeline then to the production line, also has heat leak. As the internal coolant is moving inside the cryogenic pipeline, liquid status should be guaranteed (i.e., no solidification or gasification). In general, the solidification temperature starts from 63.2 K, and the gasification temperature starts from 77.3 K. Then the normal temperature range of the liquid nitrogen should be kept between 63.2 and 77.3 K. For the uses in the proposed combo-transmission system, the above-mentioned heat leaks will cause the liquid nitrogen temperature to increase and the boiling of liquid nitrogen, and bring safety issues of high pressure in the cryogenic pipeline. From the output of valve box to aluminium extruders, if the rear coolant is mixed with liquid nitrogen and gaseous nitrogen, the actual operating temperature will be much higher than 77.3 K. For the extrusion die, the corresponding cooling power will be certainly lower than the expected value, which will finally affect the profile productivity and economic benefits.

Therefore, the combo-transmission system for 'cold energy + electricity' should properly use the functions of two gas-liquid separators to exhaust the gaseous nitrogen inside the cryogenic pipeline. The 1st gas-liquid separator isolates the gaseous nitrogen caused by the input heat leak, and only keeps the pure liquid nitrogen that can go through the cryogenic pipeline to the 2nd gas-liquid separator; similarly, the 2nd gas-liquid separator isolates the gaseous nitrogen caused by the output heat leak, and only keeps the pure liquid nitrogen that can go through the soft cryogenic pipeline and then store at the valve box. Thanks to the efforts by 2-stage gas-liquid separations, the virtually zero-loss transmission by superconducting power cable together with the cold energy delivery/circulation using pure liquid nitrogen can be realized, which is able to massively improve the energy efficiency and productivity of the aluminium production line.

4 | DESIGN AND OPTIMIZATION OF HIGH-CURRENT HTS CABLE

The superconducting material used for making the proposed high-current power cable is a commercial GdBCO tape manufactured by SuNAM. It has an average width of 12 mm and an average thickness of 0.14 mm. This superconducting tape has a really high aspect ratio (width/thickness = 85.7). As shown in Figure 3A, inside the 0.14 mm thickness, the superconducting tape uses the multi-layer deposition technology, and the actual thickness of the superconducting layer is merely 1.3 μm. During the real manufacturing process, the superconducting layer is deposited in multiple buffer layers (e.g., $LaMnO_3$, MgO, Y_2O_3, Al_2O_3) with thicknesses of 10 nm level, and all of them overlay on a 100 μm hastelloy substrate. Afterwards, both sides are first covered by 2 μm thick Ag, and then the whole body is encapsulated with 15 μm thick Cu. By measurement, this commercial superconducting tape has an average critical current of 960 A (self-field at 77 K). Considering the production line of 100 MN aluminium profile extrusion needs the stable power supply with current of 8000 A, the cable unit uses the high-current structure with parallelly stacked superconducting tapes.

Compared to conventional coaxial-type superconducting cables for long-distance power transmission,[47] the parallelly stacked tapes can be one of the most efficient structures for making short-distance high-current superconducting power cables, with the advantages of simple processing technology and compact overall size. However, considering the superconducting tape has anisotropic characteristics, the magnetic field generated by parallelly stacked tapes will directly reduce the overall critical current of the cable unit (the maximum operating current).

The critical current formula is as follows:

$$I_c\left(B_{par}, B_{perp}\right) = I_{c0} \times \left(1 + \frac{\sqrt{\gamma^{-2}B_{par}^2 + B_{perp}^2}}{B_1}\right)^{-\alpha}, \quad (1)$$

where I_{c0} is the initial critical current of the GdBCO tape at 77 K; B_{par} and B_{perp} are the parallel and perpendicular components of the external magnetic field; $B_1 = 1.592$ T,

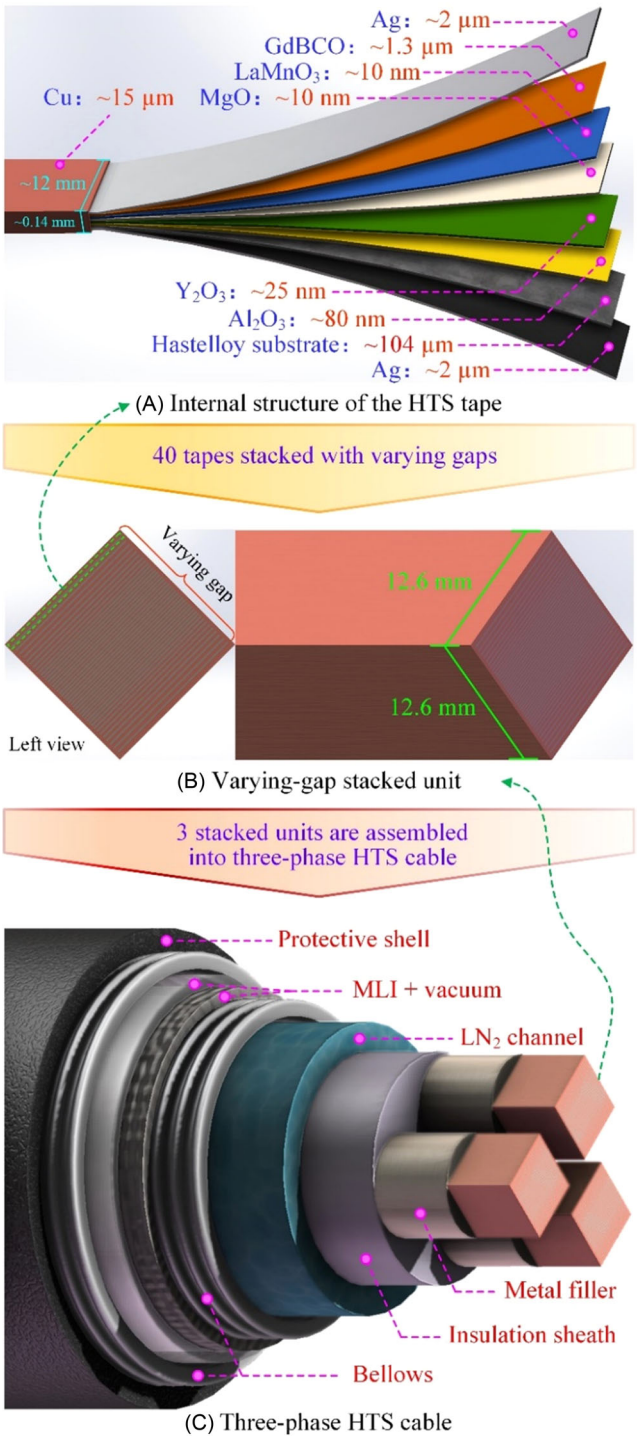

FIGURE 3 Schematic diagrams of a 10kA-class HTS power cable for the 100 MN aluminium extrusion workshop: (A) internal structure of the HTS tape, (B) varying-gap stacked unit, and (C) three-phase HTS cable. HTS, high temperature superconducting.

$\gamma = 3.383$, and $\alpha = 0.8764$ are three anisotropic factors deduced from experimental data.[48]

In this design, further optimizations are carried out using the self-programmed superconductivity tool based on the FEM package COMSOL, which is able to balance the current-carrying capability and the geometry of the HTS power cable. The field-dependent critical current modelling is carried out using the 'magnetic field, mf' package:

$$\nabla \times A = B, \tag{2}$$

$$\nabla \times H = J, \tag{3}$$

$$\mu(M + H) = B. \tag{4}$$

Equation (2) is the definition of magnetic potential: A is the magnetic potential, and B is the magnetic flux density. Equation (3) is Ampere's Law: J is the electric current density, and H is the magnetic field intensity. Equation (4) is the constitutive relationship: μ_0 is the overall permeability, and M is the magnetization. By re-arranging Equations (2)–(4), the model for the magnetic vector potential A is

$$\nabla \times \left(\frac{1}{\mu}\nabla \times A\right) = J. \tag{5}$$

The overall area of a single unit is set as a square with the side of 1.05 times of the superconducting tape width, to achieve reasonable compactness. Figure 3B shows the optimization can take advantage of the whole cross-section. Due to the maximum critical current of a single unit being strongly associated with the gaps between each tape, the end tapes are more crucial to decide the final critical current. Varying-gap optimization has been executed with an initial gap (0.2 mm) among adjacent tapes. The two-step optimizing implementations cover the Stage-1 optimization which modifies the gaps between middle HTS tapes (20 tapes in the middle) with a factor 25%, and then the Stage-2 optimization modifies the gaps between end HTS tapes (10 + 10 tapes, in both ends) with an increasing factor 10%. After the two-step optimizations, the critical current of the cable unit improves from 9302 to 9650 A by the Stage-1 optimization, and further to 9841 A by the Stage-2 optimization. Parameters of the two-step optimizations are presented in Table 1.

5 | ENERGY PIPELINE DESIGN AND PERFORMANCE ANALYSIS

The section above describes the optimization of the high-current structure with parallelly stacked superconducting tapes. For use in the 100 MN aluminium profile extrusion workshop, the rated power and rated current are 3 MW and 7894 A, respectively. The proposed cable design has a 10 kA allowable current capacity, which is

TABLE 1 Parameters for the optimized single cable unit

Parameters	Value
Number of 12-mm GdBCO tapes	40
Single-unit size (cross-section)	1.26 cm × 1.26 cm
Gap width	0.2–1.8 mm
Operating temperature	77 K
Single-tape critical current	960 A
Single-unit critical current	9841 A

higher than the rated current and can properly satisfy the power supply for the whole production line. Meanwhile, the cross-section of single cable unit is merely 12.6 mm × 12.6 mm, with the current density up to 62 A/mm^2. Comparatively, the typical current density of a conventional copper cable is only 2 A/mm^2, and the cross-section will be more than 30 times larger if taking the same current.

Since the HTS cables cannot be massively bent like copper cables, the question of how to transport and install the entire cable should be properly considered. To make a three-phase AC HTS cable unit, the optimized 10 kA single cable units and other cryogenic pipeline structures should be integrated as an assembly. Figure 3C shows the configuration of the three-phase cable with detailed cryogenic pipeline structures. First, 3 square shape cable units are encapsulated with metal fillers (e.g., aluminium), transforming from square to round shape. After that, 3 round shape cable units are nested into the insulation sheath, with each having a 120 degree phase difference and also a physical position difference. As shown in Figure 4, the distance between the circle centre of the insulation sheath and the edge of the cable units is 1.4√2 mm, and the radius of the insulation sheath r_{IS} is 14√2 mm.

During the actual cable productions, the thermal expansion coefficients of the HTS tape substrate and the metal/non-metal fillers can be matched to specific designs with reasonable safety margins. It should be note that the parallelly stacked HTS cables with these fixed configurations will loss a certain amount of flexibility, which are different from those conventional coaxial cables with good flexibility. However, for this proposed study on the applications of aluminium extrusion workshop, the transmission distance of the HTS cable is very short and the cabling is straight, and thus extremely good flexibility is not required.

After the insulation sheath (with the three-phase HTS cable) is embedded into the cryogenic pipeline, the liquid nitrogen flowing domain is established between the outer wall of the insulation sheath and the inner wall of the

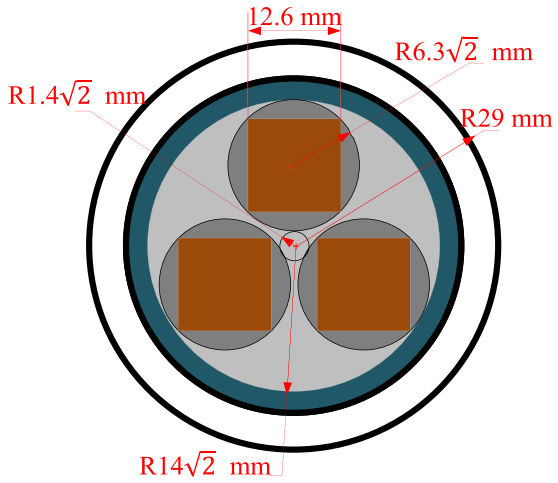

FIGURE 4 Cross-section of the three-phase HTS power cable inside the cryogenic pipeline. HTS, high temperature superconducting.

cryogenic pipeline. The structure of the proposed 3-phase HTS cable uses the round shape insulation layer, which can make good insulation between each phase, but also can integrate these three phases of round cables into a unit for easy installation and convenient transportation. Considering the insulation material has low thermal conductivity, the outermost insulation layer (exposed to LN_2) can be perforated to achieve the spot-slotted supporting structure. This special structure can ensure good LN_2 cooling effect and also strong mechanical performance.

For the cryogenic pipeline inserted with an additional HTS power cable, the effective cross-sectional area of the liquid nitrogen channel can be calculated by

$$S = \pi \times r_{pipe}^2 - \pi \times r_{IS}^2, \tag{6}$$

where r_{pipe} is the inner radius of the cryogenic pipeline, r_{IS} is the outer radius of the insulation sheath.

For this 100 MN aluminium extrusion workshop, the total consumption of liquid nitrogen in 1 year is about 1431.9 tonnes. Assuming that the workshop is operated in the 'all-day' mode, and then the volumetric flow rate Q_{LN2} required inside the cryogenic pipeline should be about 3.75 L/min. For this case, the required flow rate u of the liquid nitrogen can be determined by

$$u = \frac{Q_{LN2}}{\pi \times r_{pipe}^2 - \pi \times r_{IS}^2}. \tag{7}$$

Figure 5 shows the relationship between the flow rate of the liquid nitrogen and the inner radius of the cryogenic pipeline. From the point of view of engineering applications, a common flow rate of the liquid nitrogen is

set as 0.7 m/s, and thus the corresponding inner radius r_{pipe} is about 20.5 mm for the cryogenic pipeline. To drive the liquid nitrogen inside the cryogenic pipeline, a commercial long-shaft pump (BNCP-30-000) manufactured by Barber-Nichols Company can be used for actual operations.[49] It has a pump housing and an impeller that is submerged into the cryogenic liquid nitrogen, which is separated from the motor by an extended driveshaft.

In addition, the structure of in-cable cryostat is different from the typical smooth-faced structure of cylindrical cryostats for superconducting magnets. To meet the thermal expansion/contraction and flexibility, both the inner and outer pipes use the corrugated structure (bellows), as shown in Figure 3C. The inner and outer corrugated bellows have a certain flexibility and expansibility, which are favourable for installing the whole HTS cable from electricity distribution station to the aluminium extrusion workshop. The space between the inner and outer pipes is vacuumed below 10^{-2} Pa, to reduce thermal convection and conduction. The thermal propagation through cryostat walls from the room temperature to liquid nitrogen depends on the quantity of the multi-layer insulation (MLI). A typical MLI material composed of 25 μm alluminized polyester film and 60 μm glass fibre cloth is wound on the inner bellows of the cryostat. The number of layers is 25, and the total thickness is about 2.2 mm. For the 10 kA class three-phase HTS cable in this work, the thicknesses of vacuum space, and the inner/outer steel wall are set as 5 and 2 mm.

For the energy loss estimation, although the HTS cable itself does not have any resistive loss (excluding AC loss), the heat leakage of the current leads from the HTS cable terminals to the room-temperature environment is inevitable. If using an optimized heat leakage value of 50 W/kA for each cable terminal,[50] the proposed three-phase HTS cable has a maximum power loss of 23,682.0 W when considering a typical coefficient of performance (COP) of cryogenic refrigerator of 0.1. By comparison, a conventional copper cable is normally with a resistivity of 0.02 μΩ m and a current density of 2 A/mm^2, resulting in a unit loss of 0.08 μW m/mm^2. For a 54 m copper cable used in the 100 MN aluminium profile extrusion workshop with its power demand of 3 MW as usual, the total power loss of the copper cable is estimated about 51153.1 W. This means that the total energy loss of superconducting transmission is about 46% of conventional copper cable, as shown in Figure 6.

Figure 7 presents cross-sectional area comparisons: the new combo-transmission scheme (cold energy + electricity) versus the conventional transmission scheme using the separate electricity transmission (using a conventional copper cable), and the liquid nitrogen delivery using an independent cryogenic pipeline. The high current density in HTS tapes also leads to a very compact cable for high-dense power supply. The cross-sectional area of the whole HTS cable, including the cryogenic pipeline, is merely 2732.6 mm^2, which is much smaller than the size of an equivalent copper power cable (16,682.7 mm^2, copper conductors + insulation/wrapping materials).

Moreover, the couple of the liquid nitrogen pipeline and HTS cable make the whole system have electricity and cold energy delivery to be more compact. There is no need to build another liquid nitrogen pipeline (5 mm radius, cross-section 615.4 mm^2), and new system can also save space for installing the 16,067.3 mm^2 copper cable using another route. More importantly, every year the new system can save 240.6 MWh power consumption as there is no resistive loss in the HTS power cable, and also can prevent the safety issues of the insulation

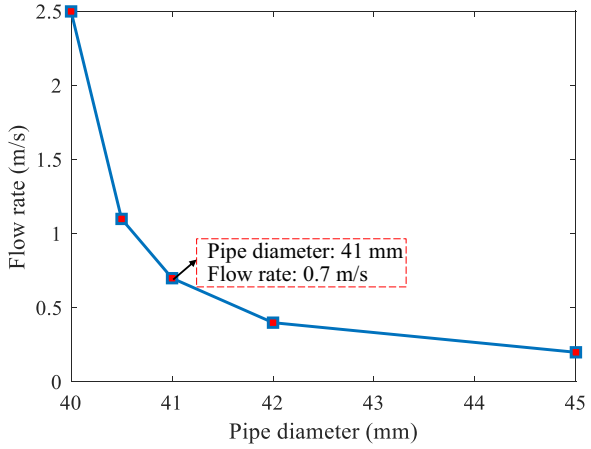

FIGURE 5 Relationship between the flow rate and inner radius of the cryogenic pipeline to accommodate the three-phase HTS cable. HTS, high temperature superconducting.

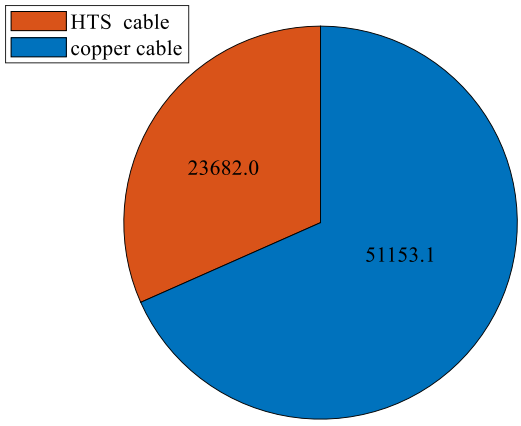

FIGURE 6 Opeating loss comparison between the HTS cable and copper cable. HTS, high temperature superconducting.

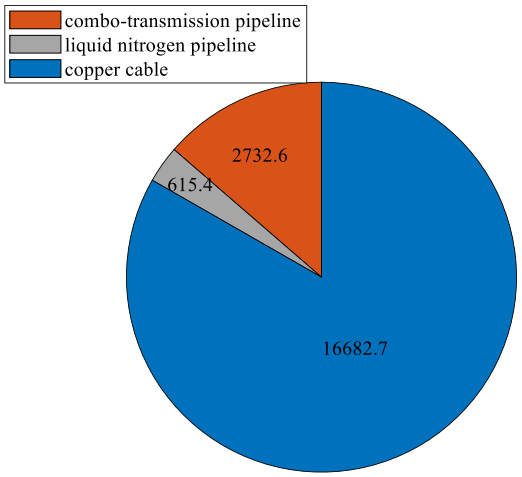

FIGURE 7 Cross-sectional area comparisons among the copper power cable, standalone liquid nitrogen pipeline and the proposed combo-transmission system for 'cold energy + electricity'.

breakdown and fire hazard caused by the over-heat of conventional copper cables suffering huge conduction loss.

6 | ECONOMIC ANALYSIS OF A 100 MN ALUMINIUM EXTRUSION PRODUCTION LINE USING LIQUID NITROGEN AND SUPERCONDUCTOR TECHNOLOGIES

According to recent market research, the average aluminium profile production of a 100 MN aluminium extrusion production line is about 9000 tons a year. If the proposed liquid nitrogen cooling scheme is used in the production line, the production output can increase by 23% according to the actual testing data in Stratton.[24] Given that a typical income for extruding the 6063-type profile is \$800 per ton, the increased gross profit W_{gross} is up to 1656 k\$ in a year. Ignoring the labour and maintenance costs, the net profit W_{net} can be estimated by

$$W_{\text{net}} = W_{\text{gross}} - C_1 - C_2, \tag{8}$$

where C_1 and C_2 are two types of liquid nitrogen cost under the conditions of cooling the aluminium profile die or compensating the heat leakage. It should be noted that the liquid nitrogen consumption K_{LN2} is about 129.35 kg for producting 6063-type profile per ton, then the first part of liquid nitrogen cost can be calculated by

$$C_1 = C_{\text{unit}} K_{LN2}(1 + S_{6063}) \times 10^{-3}, \tag{9}$$

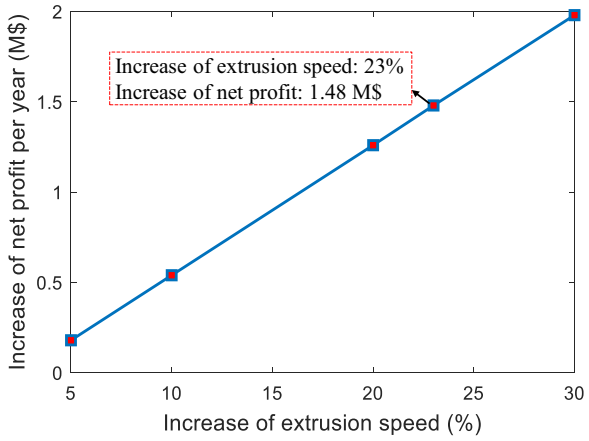

FIGURE 8 Relationship between the net profit increased per year and the increase of extrusion speed

where C_{unit} is the unit cost for purchasing the liquid nitrogen, 100 \$ per ton; S_{6063} is the proportion of the increase in extrusion speed.

For the second part of liquid nitrogen cost, it is mainly from the heat leakage of the cryogenic pipeline. When the proposed HTS cable is installed into the liquid nitrogen pipeline, three pairs of cable terminals can generate about 2368.2 W heat leakage during normal operations. This kind of heat leakage results in a certain amount of gasification of liquid nitrogen, and the corresponding liquid nitrogen cost can be calculated by

$$C_2 = C_{\text{unit}} \frac{P_{\text{heat}} t_{\text{op}}}{H_{\text{unit}}} \times 10^{-3}, \tag{10}$$

where P_{heat} is the heat leakage from the cryogenic pipeline to the room-temperature environment; t_{op} is the actual operating duration in a year; H_{unit} is the latent heat of the liquid nitrogen, 199.5 kJ/kg.

Figure 8 shows the relationship between the net profit and the increase of extrusion speed. For the 100 MN aluminium extrusion production line, the net profit increases almost linearly with the increases of the extrusion speed. For the case of 23% increase in extrusion speed, the net profit can be up to 1.48 M\$ in 1 year.

7 | CONCLUSION

In this article, a new combo-transmission scheme has been investigated for simultaneously transporting the liquid-nitrogen-based cold energy and the superconductor-based electric energy using the same cryogenic energy pipeline. The technical feasibility and economic practicality of this new energy pipeline have

been discussed and verified in a case study of a 100 MN aluminium extrusion workshop. Based on the state-of-the-art commercial tapes, a 10kA-class superconducting power cable has been designed and optimized. The designed superconducting power cable has extremely superior performance regarding the compactness (83.6% smaller than the copper cable), and energy loss (54% smaller than the copper cable). For the economic analysis, when the liquid nitrogen cooling scheme is applied for the 100 MN production line, the production output can be well expected to increase by 23%, and the corresponding net profit is 1.48 M$ in a year. To conclude, the proposed combo-transmission scheme (cold energy + electricity) using liquid nitrogen and superconductor technologies has great potential to enhance both the energy efficiency and production benefit for an actual aluminium profile extrusion workshop.

ACKNOWLEDGEMENT

This work was supported by the Sichuan Science and Technology Program (Grant No. 2022YFG0304).

ORCID

Xiaoyuan Chen http://orcid.org/0000-0002-9816-6724
Mingshun Zhang http://orcid.org/0000-0002-9149-5373
Boyang Shen http://orcid.org/0000-0001-8169-6588

REFERENCES

1. Güley V, Khalifa NB, Tekkaya AE. The effect of extrusion ratio and material flow on the mechanical properties of aluminium profiles solid state recycled from 6060 aluminium alloy chips. *AIP Conf Proc*. 2011;1353(1):1609-1614.
2. Sverdrup HU, Ragnarsdottir KV, Koca D. Aluminium for the future: modelling the global production, market supply, demand, price and long term development of the global reserves. *Resour Conserv Recy*. 2015;103:139-154.
3. Guo Y, Yu Y, Ren H, Xu L. Scenario-based DEA assessment of energy-saving technological combinations in aluminum industry. *J Clean Prod*. 2020;260:121010.
4. Ministry of Industry and Information Technology of the People's Republic of China. *Operation of aluminum industry in 2021*. https://www.miit.gov.cn/jgsj/ycls/gzdt/art/2022/art_25596e30ab6e4d9fac64f62418134ae9.html
5. National Development and Reform Commission. The relevant responsible comrades of the National Development and Reform Commission answered the reporter's questions on the Notice on Improving the Step Price Policy for the Electrolytic Aluminum Industry. https://www.ndrc.gov.cn/xxgk/jd/jd/202108/t20210827_1294977.html
6. China Nonferrous Metals Industry Association Aluminum Branch. *2021 Annual Report of Guangdong Haomei New Materials Co. Ltd*. https://www.metalchina.com/contentList?articleColumnId=7e6e6b085ae94e40b20e86ffcb0a8633&category=%26met
7. Sheppard T. *Extrusion of Aluminium Alloys*. Springer Science & Business Media; 1999.
8. Saha PK. *Aluminium Extrusion Technology*. ASM International; 2000.
9. Das AK. Special features of process defects in aluminium alloy extrusions. *Proceedings of the Fourth International Extrusion Technology Seminar*. 1988;2:11-14.
10. Parson NC, Jowett CW, Pelow CV, Fraser WC. Surface defects on 6xxx alloy extrusions. *Proceedings of International Aluminium Extrusion Technology Seminar*. 1997;1:57-68.
11. Qamar SZ, Arif AFM, Sheikh AK. Analysis of product defects in a typical aluminum extrusion facility. *Mater Manuf Process*. 2004;19(3):391-405.
12. Qamar S, Pervez T, Chekotu J. Die defects and die corrections in metal extrusion. *Metals*. 2018;8(6):380.
13. Akhtar SS, Arif AFM. Fatigue failure of extrusion dies: effect of process parameters and design features on die life. *J Fail Anal Prev*. 2010;10(1):38-49.
14. Saha PK. Thermodynamics and tribology in aluminum extrusion. *Wear*. 1998;218(2):179-190.
15. Hölker R, Jäger A, Ben Khalifa N, Tekkaya AE. Controlling heat balance in hot aluminum extrusion by additive manufactured extrusion dies with conformal cooling channels. *Int J Precis Eng Manuf*. 2013;14(8):1487-1493.
16. Hölker R, Tekkaya AE. Advancements in the manufacturing of dies for hot aluminum extrusion with conformal cooling channels. *Int J Adv Manuf Technol*. 2016;83(5):1209-1220.
17. Hölker R, Haase M, Ben Khalifa N, Tekkaya AE. Increased productivity in hot aluminum extrusion by using extrusion dies with inner cooling channels manufactured by rapid tooling. *Key Eng Mater*. 2014;611-612:981-988.
18. Barella S, Gruttadauria A, Gerosa R, Mainetti R, Mainetti T. Predictive tools for in-line isothermal extrusion of 6xxx aluminium alloys. *Mater Proc*. 2021;3(1):24.
19. Donati L, Segatori A, Reggiani B, Tomesani L, Bevilacqua Fazzini PA. Effect of liquid nitrogen die cooling on extrusion process conditions. *Key Eng Mater*. 2011;491:215-222.
20. Pachla W, Kulczyk M, Smalc-Koziorowska J, et al. Mechanical properties and microstructure of ultrafine grained commercial purity aluminium prepared by cryo-hydrostatic extrusion. *Mater Sci Eng A*. 2017;695:178-192.
21. Celani P. *Liquid nitrogen technology*. Proceedings of the 8th Aluminium Two Thousand International Congress; 2013.
22. Ward TJ, Kelly RM, Jones GA, Heffron JF. The effects of nitrogen—liquid and gaseous—on aluminium extrusion productivity. *J Met*. 1984;36(12):29-33.
23. Twigg R, Oesterreich R. Extrud-AlTM—An alternative approach to nitrogen die cooling. *Proceedings of the 8th International Extrusion Technology Seminar*. 2004:18-21.
24. Stratton P. Raising productivity of aluminium extrusion with nitrogen. *Int Heat Treat Surf Eng*. 2008;2(3-4):105-108.
25. Ciuffini A, Barella S, Di Cecca C, et al. Surface quality improvement of AA6060 aluminum extruded components through liquid nitrogen mold cooling. *Metals*. 2018;8(6):409.
26. Mazur M, Brincat P, Leary M, Brandt M. Numerical and experimental evaluation of a conformally cooled H13 steel injection mould manufactured with selective laser melting. *The Int J Adv Manuf Technol*. 2017;93(1):881-900.

27. Armillotta A, Baraggi R, Fasoli S. SLM tooling for die casting with conformal cooling channels. *Int J Adv Manuf Technol*. 2014;71(1):573-583.
28. Pelaccia R, Negozio M, Donati L, Reggiani B, Tomesani L. Extrusion of light and ultralight alloys with liquid nitrogen conformal cooled dies: process analysis and simulation. *J Mater Eng Perform*. 2022;31(3):1991-2001.
29. Pelaccia R, Negozio M, Donati L, Reggiani B, Tomesani L. Efficiency of conformal cooling channels inserts for extrusion dies. *Proce Manuf*. 2020;47:209-216.
30. Reggiani B, Donati L. Prediction of liquid nitrogen die cooling effect on the extrusion process parameters by means of FE simulations and experimental validation. *J Manuf Process*. 2019;41:231-241.
31. Pelaccia R, Reggiani B, Negozio M, Donati L. Liquid nitrogen in the industrial practice of hot aluminium extrusion: experimental and numerical investigation. *Int J Adv Manuf Technol*. 2022;119(5):3141-3155.
32. Pelaccia R, Negozio M, Reggiani B, Donati L, Tomesani L. Analysis and optimization of cooling channels performances for industrial extrusion dies. 24th International Conference on Material Forming. 2021.
33. Hölker R, Jäger A, Ben Khalifa N, Tekkaya AE. New concepts for cooling of extrusion dies manufactured by rapid tooling. *Key Eng Mater*. 2011;491:223-232.
34. Hölker R, Haase M, Khalifa NB, Tekkaya AE. Hot extrusion dies with conformal cooling channels produced by additive manufacturing. *Mater Today Proc*. 2015;2(10):4838-4846.
35. Reggiani B, Todaro I. Investigation on the design of a novel selective laser melted insert for extrusion dies with conformal cooling channels. *Int J Adv Manuf Technol*. 2019;104(1):815-830.
36. Chen X, Jiang S, Chen Y, et al. Energy-saving superconducting power delivery from renewable energy source to a 100-MW-class data center. *Appl Energy*. 2022;310:118602.
37. Chen X, Jiang S, Chen Y, et al. A 10 MW class data center with ultra-dense high-efficiency energy distribution: design and economic evaluation of superconducting DC busbar networks. *Energy*. 2022;250:123820.
38. Chen X, Zhang M, Jiang S, et al. Energy reliability enhancement of a data center/wind hybrid DC network using superconducting magnetic energy storage *Energy*. 2023;263:125622.
39. Yuan W, Venuturumilli S, Zhang Z, Mavrocostanti Y, Zhang M. Economic feasibility study of using high-temperature superconducting cables in UK's electrical distribution networks. *IEEE Trans Appl Supercond*. 2018;28(4):1-5.
40. Yazdani-Asrami M, Seyyedbarzegar S, Sadeghi A, de Sousa WTB, Kottonau D. High temperature superconducting cables and their performance against short circuit faults: current development, challenges, solutions, and future trends. *Supercond Sci Technol*. 2022;35(8):083002.
41. Terazaki Y, Yanagi N, Ito S, et al. Measurement and analysis of critical current of 100-kA class simply-stacked HTS conductors. *IEEE Trans Appl Supercond*. 2014;25(3):4602905.
42. Kang R, Uglietti D, Wesche R, Sedlak K, Bruzzone P, Song Y. Quench simulation of REBCO cable-in-conduit conductor with twisted stacked-tape cable. *IEEE Trans Appl Supercond*. 2019;30(1):5700107.
43. Li Y, Wang YS, Miao JY, et al. Investigation on critical current properties of quasi-isotropic strand made from coated conductors. *IEEE Trans Appl Supercond*. 2014;25(3):6600805.
44. Van der Laan DC, Noyes PD, Miller GE, Weijers HW, Willering GP. Characterization of a high-temperature superconducting conductor on round core cables in magnetic fields up to 20T. *Supercond Sci Technol*. 2013;26(4):045005.
45. Komeda T, Amemiya N, Tsukamoto T, et al. Experimental comparison of AC loss in REBCO roebel cables consisting of six strands and ten strands. *IEEE Trans Appl Supercond*. 2013;24(3):8200505.
46. Shi Y, Liu F, Liu H, et al. Quasi-round HTS conductor using REBCO tapes for fusion magnet application. *IEEE Trans Appl Supercond*. 2020;30(1):1-4.
47. Chen Y, Jiang S, Chen XY, Wang YF, Li T. Preliminary design and evaluation of large-diameter superconducting cable toward GW-class hybrid energy transfer of electricity, liquefied natural gas, and liquefied nitrogen. *Energy Sci Eng*. 2020;8(5):1811-1823.
48. Shen B, Grilli F, Coombs T. Review of the AC loss computation for HTS using H formulation. *Supercond Sci Technol*. 2020;33(3):033002.
49. Barber-Nichols Company. *Cryogenic pumps*. https://www.barber-nichols.com/products/pumps/cryogenic-pumps/liquid-nitrogen-pumps/
50. Yamaguchi S, Koshizuka H, Hayashi K, Sawamura T. Concept and design of 500 meter and 1000 meter DC superconducting power cables in Ishikari, Japan. *IEEE Trans Appl Supercond*. 2015;25(3):1-4.

How to cite this article: Chen X, Li Q, Jiang S, Zhang M, Fu L, Shen B. A novel combo-transmission system of cold energy and electricity for aluminium profile production: using liquid nitrogen and superconductor technologies. *Energy Sci Eng*. 2022;1-11. doi:10.1002/ese3.1378